Chemical potential of vibrations and its driven energy transport in hybrid nano-junctions

Lei-Lei Nian and Jing-Tao Lü*

School of Physics and Wuhan National High Magnetic Field Center,

Huazhong University of Science and Technology, Wuhan 430074, P. R. China

(Dated: July 24, 2019)

Abstract

Abstract...

* jtlu@hust.edu.cn

I. INTRODUCTION

Quantum transport in nanoscale systems is well described by the celebrated Landauer-Büttiker approach. It has been successfully used to study charge, energy and their coupled transport carried by particles following different statistics, including electrons[], photons[1], and phonons[2–8]. The energy current between two baths ($i = 1, 2$) can be written as the following general form

$$J = \int_0^{+\infty} \frac{d\omega}{2\pi} \hbar\omega T(\omega)[n(\omega, \mu_1, T_1) - n(\omega, \mu_2, T_2)], \tag{1}$$

where the key quantity is the transmission coefficient $T(\omega)$. The distribution function n is determined by the particle statistics. For fermions, it is the Fermi-Dirac distribution. Either a chemical potential or a temperature bias can driven an energy current flow. Thus, thermoelectric transport can also be studied using this approach. For bosons, n is the Bose-Einstein distribution. Equation 1 has been used to study temperature-driven energy transport carried by phonons, photons and other quasi-particles. Here, we have $\mu = 0$, following the textbook argument that bosons without number conservation have zero chemical potential. Thus, for bosonic energy transport the only driving force is temperature.

However, the generation and annihilation of bosons may be accompanied by transitions between different states of particles with non-zero chemical potentials. This is certainly the case for electrically driven processes. In such situations, it is known that the chemical potential of bosons does not have to be zero. In thiw work, we show that, energy transport between nonequilibrium electrons and bosons can be well described by the Landauer formula between bosonic baths with different chemical potential. The key observation is that, the electronic system can be treated as bosonic electron-hole-pair bath with non-zero chemical potential.

II. SYSTEM

We consider a model system schematically shown in Fig. **??**. The center system composed of bosonic degrees of freedom (DOF) couples to two kinds of baths. One is an equilibrium boson bath, modeled by harmonic oscillators. The other is an electronic bath possibly driven into nonequilibrium steady state by voltage bias applied between two electrodes. The electronic bath is further divided into two electrodes and one center region. The bosonic

system couples only to the center region of the electronic bath. Energy transport from the electron bath to the system is realized through this coupling. The energy injected into (substracted from) the system can further goes into (out of) the harmonic oscillator bath. The above model is quite general. To be more specific, we consider a molecular junction as an example. Applications of this model include current-induced heating or electroluminescence. The bosonic system represents molecular vibrations and cavity photon modes, respectively.

III. ELECTRON-HOLE PAIR EXCITATIONS

Our key observation is that the interaction between the system and electron bath can be modeled by different kinds of reactions between electron hole pairs (EHPs) in the bath and the bosonic modes in the system. The creation and annihilation of the bosonic mode is always accompanied by the recombination and creation of EHPs, expressed in the form of reactions

$$e_\alpha + h_\beta \rightleftharpoons p_n, \tag{2}$$

where e_α, h_β and p represent electron in electrode α, hole in electrode β and bosonic mode n in the system. There are four types of EHPs which we label by the spatial location of the electron (α) and hole (β) state. They are schematically shown in Fig. 1. In additional to energy transfer between electron bath and the system, the generation and recombination of inter-electrode EHPs ($\alpha \neq \beta$) involves electron transport between the two electrodes. Physically, the reaction in Eq. (2) involves inelastic electronic transition assisted by the bosonic mode.

The coupling-weighted EHP power spectrum can be written as

$$\Lambda^{\alpha\beta}(\omega) = \hbar\omega \left(n_B(\hbar\omega - \mu_{\alpha\beta}, T_e) + \frac{1}{2} \right) \Gamma^{\alpha\beta}(\omega), \tag{3}$$

with the coupling weighted density of states (DOS)

$$\begin{aligned} \Gamma^{\alpha\beta}(\omega) = & -\sum_{i_\alpha, f_\beta} |\langle \psi_{i_\alpha}(\varepsilon_i) | M^n | \psi_{f_\beta}(\varepsilon_f) \rangle|^2 \delta(\varepsilon_i - \varepsilon_f - \hbar\omega) \\ & \times (n_F(\varepsilon_\alpha - \mu_\alpha, T_\alpha) - n_F(\varepsilon_\beta - \mu_\beta, T_\beta))(\hbar\omega)^{-1} \qquad (4) \\ = & -\int d\varepsilon_\alpha \mathrm{tr}[M^n A_\beta(\varepsilon - \hbar\omega) M^n A_\alpha(\varepsilon_\alpha)] \\ & \times (n_F(\varepsilon_\alpha - \mu_\alpha, T_\alpha) - n_F(\varepsilon_\beta - \mu_\beta, T_\beta))(\hbar\omega)^{-1} \qquad (5) \end{aligned}$$

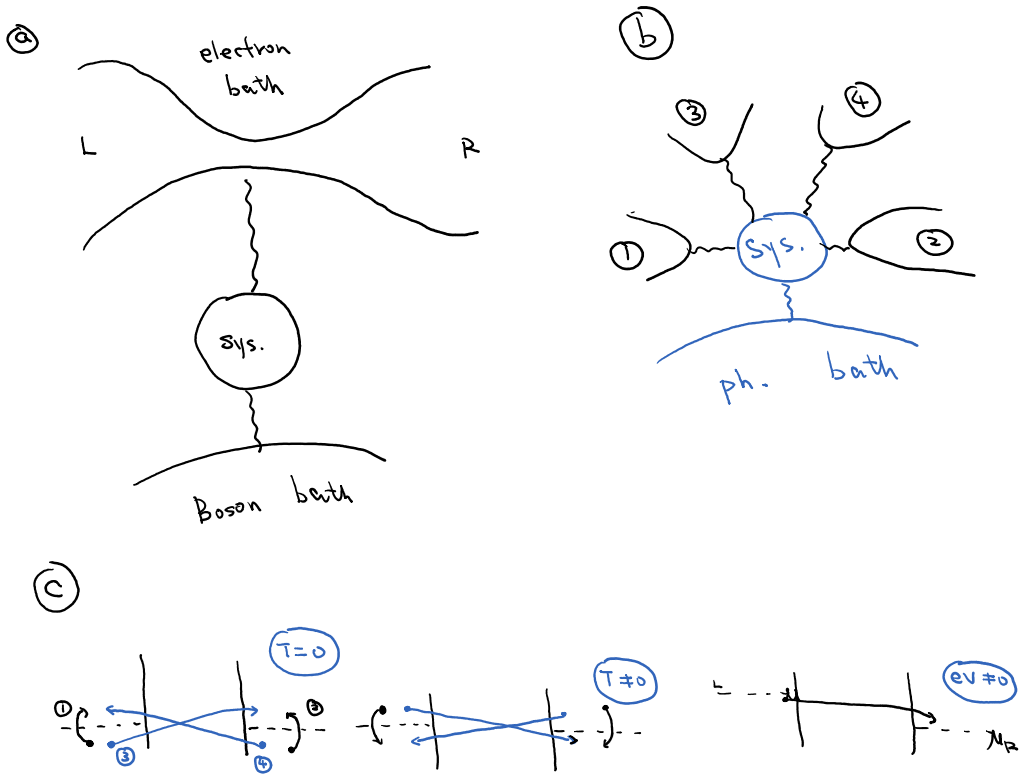

FIG. 1. (a) Schematics of the model we consider. The system consists a set of independent bosonic modes. It couples to an electron bath, which is modeled as a conductor including a left (L) and a right (R) electrode, with temperature T_e and chemical potential μ_L and μ_R, respectively. The system further couples to an external thermal bath (ph bath) at temperature T_{ph}. (b) The electron bath can be treated as four different kinds of electron-hole pair (EHP) baths (1-4). (c) Four kinds of EHP excitation at different situations. The EHPs are classified according to the spatial location of the electron and hole. (1) Both are at electrode L, (2) Both are at electrode R, (3) The electron is at electrode L is excited and transferred to electrode R. (4) The electron at electrode R is excited and transferred to the left. (d) At $T \neq 0$, the recombination of EHPs becomes possible due to the non-zero filling of electrons above the chemical potential. (e) In the presence of voltage bias an extra inter-electrode EHP recombination channel opens.

Here, n_F and n_B are the Fermi-Dirac and the Bose-Einstein distributions, respectively,

$$n_{F/B}(\varepsilon, T) = \frac{1}{\exp\left(\frac{\varepsilon}{k_B T}\right) \pm 1}, \tag{6}$$

and $\mu_{\alpha\beta} = \mu_\alpha - \mu_\beta$. Equation 3 shows that the EHP follow Bose-Enistein statistics, since it consists of two fermions. Interestingly, its chemical potential is determined by the difference

of electron and hole electrochemical potential. In equilibrium, both electrodes have the same chemical potential, thus $\mu_{\alpha\beta} = 0$. However, when there is a voltage bias, inter-electrode EHPs acquire a non-zero chemical potential, which can be the driving force for energy transport to the system.

IV. ENERGY TRANSPORT

To study energy transport in our system, we can employ a simple model using the EHP picture. The electron bath is divided into four EHP baths, each of which is characterized by the power spectra given in Eq. (3). To the lowest order approximation, we arrive at a Landauer-Büttiker formula for the energy transport from electron bath to bosonic system as a summation of contributions from all the EHP baths

$$J = \sum_{\alpha,\beta} \int_0^{+\infty} \frac{d\omega}{2\pi} \hbar\omega \; T^{\alpha\beta}(\omega) \times [n_B(\omega - \mu_{\alpha\beta}, T_e) - n_B(\omega, T_{ph})] \tag{7}$$

where

$$T^{\alpha\beta}(\omega) = \mathrm{Tr}[\Gamma^{\alpha\beta}(\omega)\mathcal{A}(\omega)], \tag{8}$$

is the transmission between the EHP bath $\alpha\beta$ and the ph-bath. Here, α,β are indices for the electron baths, T_e and T_{ph} are the temperature of the electron and harmonic-oscillator baths, resepctively. The trace Tr is over system DOF, with $\mathcal{A}_{ph} = D^r \Gamma_{ph} D^a$ the spectral function of the system due to coupling to the ph-bath. The summation over $\alpha\beta$ includes contributions from all the four types of EHPs. In the following we discuss several applications of the central result.

A. Heat Rectification in hybrid electron-boson system

Firstly, we consider the situation where the electron and phonon baths are in their own equilibrium with two different temperature T_e and T_{ph}. Since $\mu_\alpha = \mu_\beta$ and $T_\alpha = T_\beta = T_e$, we can write the total EHP DOS as an integral form

$$\Gamma(\omega) = -\frac{1}{\hbar\omega} \int d\varepsilon_\alpha \mathrm{tr}[M^n A(\varepsilon - \hbar\omega) M^n A(\varepsilon)] \times (n_F(\varepsilon - \mu_e, T_e) - n_F(\varepsilon - \hbar\omega - \mu_e, T_e)) \tag{9}$$

If we ignore the energy dependence of A, the integral of the two Fermi-Dirac distributions gives $\hbar\omega$ independent of T_e. Consequently, $\Gamma(\omega)$ does not depend on T_e. Equation (**??**) reduces to the Landauer formula for heat transport between two harmonic oscillator baths. On the other hand, if we consider the energy dependence of $A(\omega)$, $\Gamma(\omega)$ will depend on T_e. Then, heat rectification is possible $J(\Delta T) \neq J(-\Delta T)$, with $\Delta T = T_e - T_{ph}$. Thus, a necessary condition for heat rectification in a hybrid electron-boson system is that, the electron DOS near the electrochemical potential has to be energy dependent[9, 10].

B. Electronic heating and cooling

If there is a voltage bias applied between the two electrodes, the inter-electrode EHPs acquire a non-zero chemical potential, determined by the electrochemical potential difference between the two electrodes. We assume $\mu_L > \mu_R$ without loss of generality. The EHP-4 has a chemical potential of $eV = \mu_L - \mu_R$, while EHP-3 gets a chemical potential with oppositve value $-eV$. This change of the chemical potential breaks the chemical equilibrium in the reaction, and drives the energy transport between the electron bath and bosonic system. The forward reaction $e_L + h_R \rightarrow p_n$ is enhanced, leading to energy flow from the EHPs to the bosonic mode. Meanwhile, that of $e_R + h_L \rightarrow p_n$ is reduced, leading to an opposite energy flow. Direction of the total energy current is determined by the relative magnitude of the two processes, i.e., the magnitude of the transmission $T^{\alpha\beta}$. As an illustration, we consider electronic cooling of the bosonic mode.

V. MODE POPULATION AND CHEMICAL POTENTIAL

The reaction 2 suggests that, when reaching steady state, the bosonic mode created from the EHPs inherits the chemical potential of the EHPs. Thus, the bosonic mode may have a non-zero chemical potential. This is best illustrated by performing a mode population analysis.

To simplify the analysis, we consider one bosonic mode with angular frequency Ω. A simple master equation for the mode population can be established by considering the creation and annihilation processes

$$\dot{N} = B(N+1) - AN, \tag{10}$$

where B and A are the coefficients for mode creation and absorption processes. They can be calculated using the standard Fermi golden rule approach[11]. The steady state population is obtained by setting $\dot{N} = 0$ as

$$N = \frac{1}{A/B - 1}. \tag{11}$$

In equilibrium, detailed balance requires $A/B = exp(\hbar\Omega/k_BT)$. Thus N follows the standard Bose-Einstein distribution with temperature T_e and zero chemical potential. When there is bias applied, in the extreme case where the reaction rate of $e_L + h_R \to p$ is much larger than all the rest processes, the mode reaches equilibrium with EHP-4. The population still follows the Bose-Einstein distribution, but with a chemical potential eV

$$N = \frac{1}{\exp((\hbar\Omega - eV)/k_BT) - 1}. \tag{12}$$

Efficiency of a heat engine using the bononic system as working medium

$$\eta = 1 - \frac{T_L}{T_H}\frac{\hbar\Omega - eV}{\hbar\Omega} > 1 - \frac{T_L}{T_H}. \tag{13}$$

It seems that the efficiency is larger than the Carnot efficiency between T_L and T_H. The reason is that, the bosonic mode has a nonzero chemical potential, the energy input from T_H includes not only heat, but also chemical energy. All the chemical energy can be converted to work.

Appendix A: introduction

How to understand the transport phenomena in microscopic systems (such as quantum dots or wires, molecules, graphene, etc.) is a key problem. A series of theories have been developed to explain them, in which the scattering approach by Landauer[13] and Büttiker[14] is the most commonly used, termed Landauer formalism. The initial application of this formula is the noninteracting electrons, hereafter, which was extended to include the electron-Boson and electron-electron interactions[15–17]. In the Landauer formalism, the current through a two or multi- terminal device (including electrodes and a finite region) can be expressed generally by the transmission coefficient and distributions of the electrodes. This has been utilized in areas ranging from molecular electronics, spintronics to optoelectronics[18–20].

On the other hand, the Landauer-like formula for Bose system has been proposed, in which the current is driven by the temperature bias between two heat baths[1–8]. One may ask a question: *Can the current be driven by an effective chemical potential of Boson*? To answer this question, we may propose a phenomenological Landauer-like formula

$$J_B = \int_{-\infty}^{+\infty} \hbar\omega\tau(\omega)[n_L(\omega,\nu_L,T_L) - n_R(\omega,\nu_R,T_R)], \tag{A1}$$

where $\tau(\omega)$ is the transmission coefficient, $n_\alpha(\omega,\nu_\alpha,T_\alpha) = [e^{(\hbar\omega-\nu_\alpha)/k_BT_\alpha} - 1]^{-1}$ is the Bose-Einstein distribution function in bath $\alpha = L/R$ with the effective chemical potential $\nu_{L/R}$ and the temperature $T_{L/R}$. To date, the importance of Eq. (A1) has not been clarified in the quantum transport, especially in systems with electron-Boson interactions, such as electron-phonon and electron-photon.

In this paper, we will try to demonstrate that Eq. (A1) for the energy transport through coupled electron-Boson system is highly desirable. We first propose an effective model and Hamiltonian that can describe the Eq. (A1). Three examples in order to clarify the Eq. (A1) will be discussed: heat transport through a coupled electron-phonon system, light emission from single molecules, and near field thermal radiation. Moreover, the application of Eq. (A1) will be presented.

Appendix B: Model

We cosider a Bose system coupled to two heat baths, as shown in Fig. 2. The corresponding Hamiltonian takes the form

$$H = H_L + H_B + H_R + H_{LB} + H_{BR}, \tag{B1}$$

where H_L describes the left bath. It can be regarded as an effective nonequilibrium bath driven by a bias voltage, such that $T_L > 0$ and $\nu_R \neq 0$. H_R represents a equilibrium (nonequilibrium) bath with $T_R > 0$ and $\nu_R = 0$ ($\nu_R \neq 0$). H_B is the Bose system, which can be viewed as the scattering center. H_{LB} and H_{BR} represent the system-bath couplings.

In the following, we will present that the coupled electron-Boson system can be described by the effective model in Fig. 2. Specifically, the non-zero Bose chemical potential is driven by electron system with electron-Boson coupling under a bias voltage. Meanwhile, the energy transport in such systems is naturally carried out by Eq. (A1).

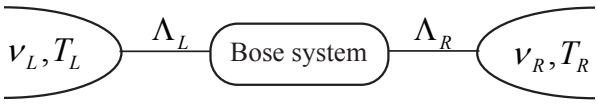

FIG. 2. Schematic view of a Bose system connected to two Bose baths. $T_{L,R}$, $\nu_{L,R}$, and $\Lambda_{L/R}$ are the temperature, the chemical potential, and the coupling bewteen system and heat bath.

Appendix C: Examples

1. Heat transport through a coupled electron-phonon system

Without loss of generality, we consider a four terminal coupled electron-phonon model, as illustrated in Fig. 3. There is a finite voltage bias between two electron bath, i.e., $\mu_e^L = eV/2$, $\mu_e^R = -eV/2$, and $T_e^L = T_e^R = T_p^L = T_p^R$. In this case, the Joule heating driven by electron-phonon interaction becomes important. By means of the nonequilibrium Green's function (NEGF) method, the energy transfer from electron to phonon system can be written as[17]

$$Q = -i \int \frac{d\varepsilon}{2\pi} \int \frac{d\omega}{2\pi} \hbar\omega \mathrm{Tr}[\mathrm{tr}[M G_0^>(\varepsilon) M G_0^<(\varepsilon - \hbar\omega)] D_0^<(\omega)]. \tag{C1}$$

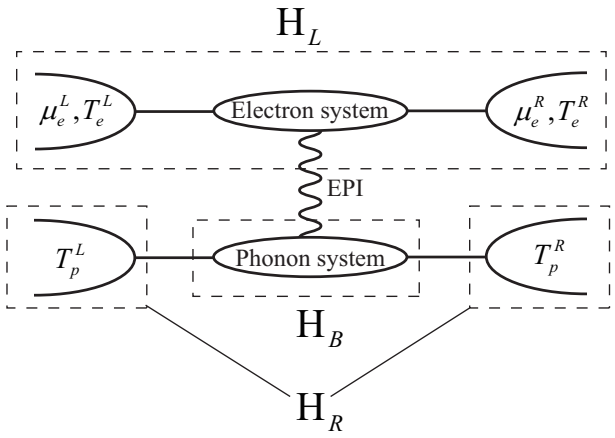

FIG. 3. A four terminal coupled electron-phonon system, in which the electron and phonon subsystem are connected by electron-phonon interaction (EPI) .

Here, G_0 and D_0 are the bare Green functions of electronic and phononic degrees of freedom, M is electron-phonon coupling matrix. By introducing the DOS and the time-reversed DOS of electrons and phonons induced by electrode $\alpha(= L, R)$[21]

$$\begin{aligned} A_\alpha(\varepsilon) &= G_0^r(\varepsilon)\Gamma_\alpha^e(\varepsilon)G_0^a(\varepsilon), \\ \tilde{A}_\alpha(\varepsilon) &= G_0^a(\varepsilon)\Gamma_\alpha^e(\varepsilon)G_0^r(\varepsilon), \\ A(\varepsilon) &= A_L(\varepsilon) + A_R(\varepsilon), \end{aligned} \tag{C2}$$

and

$$\begin{aligned} \mathcal{A}_\alpha(\omega) &= D_0^r(\omega)\Gamma_\alpha^p(\omega)D_0^a(\omega), \\ \tilde{\mathcal{A}}_\alpha(\omega) &= D_0^a(\omega)\Gamma_\alpha^p(\omega)D_0^r(\omega), \\ \mathcal{A}(\omega) &= \mathcal{A}_L(\omega) + \mathcal{A}_R(\omega). \end{aligned} \tag{C3}$$

The energy flux can be written as (see Appendix A for details)

$$Q = \int \frac{d\omega}{2\pi}\hbar\omega \mathrm{Tr}[\Lambda_{LR}\mathcal{A}(\omega)][n_B(\hbar\omega; T_p) - n_B(\hbar\omega - eV; T_e)], \tag{C4}$$

where $T_p = T_p^L = T_p^R$ and $T_e = T_e^L = T_e^R$. Eq. C4 is a phononic analog to the Landauer transport formula in nonequilibrium state, in which the driven bias is the effective chemical potential eV of Bosons. In fact, the nonequilibrium electron subsystem with electron-phonon coupling modelled by H_L in Fig. 3 satisfies a Bose distribution with an effective chemical potential, which can be obtained by means of rate equation[11].

2. Light emission from single molecules

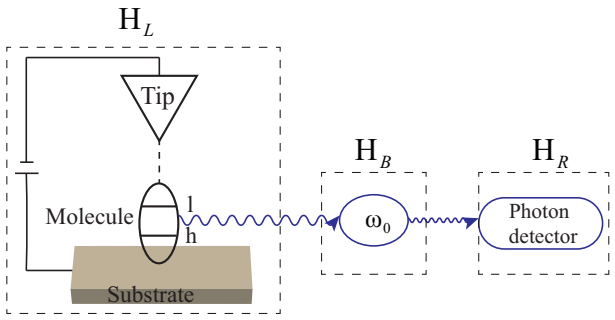

FIG. 4. STM-induced light emission from a single molecule.

In scanning tunneling microscope (STM) induced single molecule electroluminescence experiments, the light emission induced by the recombination of electrons and holes injected from STM tip and substrate has been clarified by experiment and theory[22–26]. Specifically, when a voltage bias exists between Tip and substrate, an electron and a hole will tunnel to LUMO (l) and HOMO (h) levels from Tip and substrate (see Fig. 4), such that the light emission excited by the recombination of them can be observed. Because this is no coupling between LUMO and HOMO, the energy of electrons (holes) is approximately equal to the chemical potential of Tip (substrate), that is, $\varepsilon_l = \mu_t$ and $\varepsilon_h = \mu_s$.

The process of light emission in Fig. 4 is similar to the chemical reaction, that is, the recombination of an electron (e) and a hole (h) produces a photon (p)

$$e + h \rightleftharpoons p. \tag{C5}$$

For the minimum of the free energy, we can get

$$dE = \mu_e dn_e + \mu_h dn_h + \mu_p dn_p = 0. \tag{C6}$$

where $n_{e,h,p}$ is the particle numbers of electron/hole/photon. The conservation of particle numbers requires

$$dn_e = dn_h = -dn_p. \tag{C7}$$

Finally, we have

$$\mu_e + \mu_h = \mu_p, \tag{C8}$$

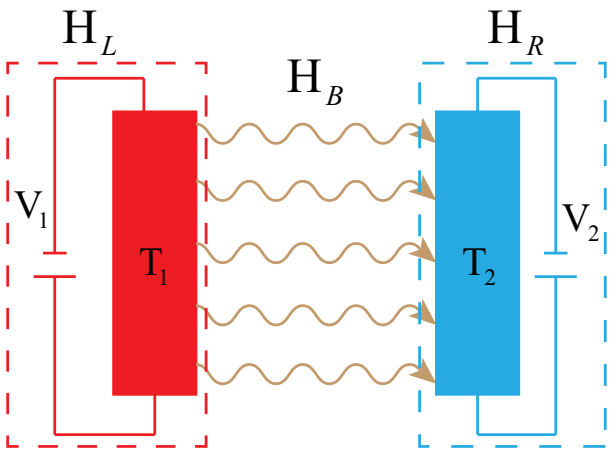

FIG. 5. Schematic of the configuration for two-body thermal radiation. V_1 (V_2) and T_1 (T_2) represent the bias voltage and temperature of the two bodies, respectively.

where μ_p is the chemical potential of photon. The sum $\mu_e + \mu_h$ is the difference $\varepsilon_e - \varepsilon_h$ of the quasi-Fermi energies of the electrons in the LUMO band and holes in the HOMO, respectively[27]. For our case, $\varepsilon_e - \varepsilon_h$ =eV.

Based on NEGF method and the Hamiltonian of the model in Fig. 4(see Appendix B), for the energy flow from the electronic system to the photonic system, we can get a Landauer-type formula similar to Eq. C4. The energy-dependent flux can be defined to study the light emission from a molecule-mediated STM juction[28].

3. Radiative heat transfer

The thermal radiation mechanism can be described by the model in Fig. 5 and can be projected into the general model in Fig. 2. In this case, the Eq. A1 with $\nu_L \neq 0$ (and $\nu_R = 0$) and $T_L = T_R \neq 0$ can be used to fitted the thermal radiation. What's more, we may predict another thermal radiation device consisting of two semiconductor p-n junctions at different external biases, as shown in Fig. 5. The thermal radiation will be flowing from the terminal with high bias to the one with low bias. This may provide a new idea to control the derection of thermal radiation.

Appendix D: Applications

In current carrying molecular junctions, the heating induced by vibrational excitation is a common process[18, 29–33]. This occurs when the molecular levels are located in the bias window and bias voltage exceeds molecular vibrational frequencies. Once the energy dissipation from molecule junction to environment is not effective enough, the temperature of the junction will be increased, leading to its instability or even breakdown. Therefore, cooling the molecular junction is important for building molecular-based electronic devices[34–36].

In Eq. C4 Q represents the energy transfer from electron to phonon subsystem. So, the phonon cooling occurs when $Q < 0$ and $T_e > T_p$. This indicates that the energy flux can flow from phonon system with low temperature to electron system with high temperature.

The optical cooling of solids driven by coherent laser light has been observed[37]. Recently, Zhu *et al.* proposed a incoherent way to control the thermal radiation in a photodiode combined with an enhanced transfer of near field thermal radiation[38]. In this experiment, the authors can adjust the chemical potential of photons to achieve the near-field photonic cooling.

In general, the nonzero chemical potential can be realized in two ways[39]: (1) The light is induced by a photochemical reaction. If the light is in chemical equilibrium with the excitations of matter (such as single molecules) whose chemical potential is nonzero, for example, the electron-hole pairs in STM junction; (2) Another way to obtain $\mu_p \neq 0$ is driven by a thermodynamic process. One can start with $\mu_p = 0$ and change the chemical potential in a thermodynamic. Once photons do not interact with matter, a zero chemical potential can be achieved.

Based on Eq. A1 and the model in Fig. 5, we can provide a more clearer explaination of the photonic cooling. As shown in Fig. 5, the chemical potentials of the cold body 2 and the hot body 1 are set to be $V_2 > 0$ and $V_1 = 0$, then a net heat flow from the cold body to the hot one can be obtained. What's more, by setting $V_1 < 0$ and $V_2 = 0$, one can observed the negative luminescence[40], and a net heat flow from cold body 2 to the hot body 1 can also be obtained.

In this case, we set the voltage bias between two electrodes is 0, that is, $\mu_e^L = \mu_e^R$. Meanwhile, a temperature bias is presented between electron and phonon subsystem, that is, $T_e^L = T_e^R \neq T_p^L = T_p^R$.

In Eq. C4, the term $[n_B(\hbar\omega;T_p) - n_B(\hbar\omega;T_e)]$ is temperature dependent. Then the effective transmission function $\mathrm{Tr}[\Lambda_{LR}\mathcal{A}(\omega)]$ is key for heat rectification. It is obviously to verify that the heat rectification vanishes when Λ_{LR} is a constant, that is, Λ_{LR} is temperature independent. Our analysis can be identified by examining the energy transport in metal-insulator interface with electron-phonon scattering[9, 10] and insulating ferromagnetic spin junction with spin-phonon interaction[41].

Appendix E: Conclusion

In summary, we have proposed a nonequilibrium Landauer formula and constructed a model for coupled electron-Boson systems. The Landauer approach developed here allows for analytical insight into the energy transport in three systems with electron-boson interaction. Moreover, the phononic cooling, photonic cooling and heat rectification can be explained clearly by the formula.

On the other hand, thermal Hall effect[42], thermal drag[43] and thermal diode[44] driven by thermal photons have been proposed theoretically. Based on the proposed nonequilibrium Landauer formula, future works may aim at achieving these transport phenomenon by introducing the 'bias-voltage-photon', that is, the photons with nonzero chemical potential driven by bias voltage.

ACKNOWLEDGMENTS

Funding is provided by the National Natural Science Foundation of China (Grant No. 21873033), the National Key Research and Development Program of China (Grant No. 2017YFA0403501) and the program for HUST academic frontier youth team.

Appendix A: Derivation of Eq. (C4)

The Hamiltonian describing the coupled electron-phonon system in Fig. (3) is

$$
\begin{aligned}
H_e^\alpha = & \underbrace{\sum_i \varepsilon_i^\alpha c_i^{\dagger\alpha} c_i^\alpha + \sum_{|i-j|=1} t_{ij}^\alpha c_i^{\dagger\alpha} c_j^\alpha + \sum_{ij} t_{ij}^{LC} c_i^{\dagger L} c_j^C + \sum_{ij} t_{ji}^{CL} c_j^{\dagger C} c_i^L + \sum_{ij} t_{ij}^{CR} c_i^{\dagger C} c_j^R + \sum_{ij} t_{ji}^{RC} c_j^{\dagger R} c_i^C}_{H_L} \\
& + \underbrace{\frac{1}{2}\sum_i \dot{u}_i^C \dot{u}_i^C + \frac{1}{2}\sum_{|i-j|=0,1} u_i^C K_{ij}^C u_j^C}_{H_B} + \underbrace{\frac{1}{2}\sum_i \dot{u}_i^\alpha \dot{u}_i^\alpha + \frac{1}{2}\sum_{|i-j|=0,1} u_i^\alpha K_{ij}^\alpha u_j^\alpha}_{H_R} + \underbrace{\sum_{ijk} M_{ij}^k c_i^\dagger c_i u_k}_{H_{LB}} \\
& + \underbrace{\frac{1}{2}\sum_{ij} u_i^L K_{ij}^{LC} u_j^C + \frac{1}{2}\sum_{ij} u_j^C K_{ji}^{CL} u_i^L + \frac{1}{2}\sum_{ij} u_i^C K_{ij}^{CR} u_j^R + \frac{1}{2}\sum_{ij} u_j^R K_{ji}^{RC} u_i^C}_{H_{BR}},
\end{aligned}
\tag{A1}
$$

where the full Hamiltonian can be divided into three parts, respectively, corresponding to the H_L, H_B, and H_R with their coupling H_{LB} in Eq. B1.

The energy flux from electron to phonon subsystem is[17, 21]

$$
Q = -i\int \frac{d\varepsilon}{2\pi}\int \frac{d\omega}{2\pi}\hbar\omega \mathrm{Tr}[\mathrm{tr}[MG_0^>(\varepsilon)MG_0^<(\varepsilon-\hbar\omega)]D_0^<(\omega)], \tag{A2}
$$

where

$$
\begin{aligned}
G_0^< &= G_0^r[\Sigma_L^< + \Sigma_R^<]G_0^a \\
&= G_0^r\Sigma_L^< G_0^a + G_0^r\Sigma_R^< G_0^a \\
&= G_0^r i\Gamma_L^e f_L G_0^a + G_0^r i\Gamma_R^e f_R G_0^a \\
&= i f_L A_L + i f_R A_R.
\end{aligned}
\tag{A3}
$$

$$
\begin{aligned}
G_0^> &= G_0^r[\Sigma_L^> + \Sigma_R^>]G_0^a \\
&= G_0^r\Sigma_L^> G_0^a + G_0^r\Sigma_R^> G_0^a \\
&= G_0^r i\Gamma_L^e (f_L-1) G_0^a + G_0^r i\Gamma_R^e (f_R-1) G_0^a \\
&= i(f_L-1) A_L + i(f_R-1) A_R.
\end{aligned}
\tag{A4}
$$

$$
\begin{aligned}
D_0^< &= D_0^r[\Pi_L^< + \Pi_R^<]D_0^a \\
&= D_0^r\Pi_L^< D_0^a + D_0^r\Pi_R^< D_0^a \\
&= -iD_0^r\Gamma_L^p n_L D_0^a - iD_0^r\Gamma_R^p n_R D_0^a \\
&= -in_L\mathcal{A}_L - in_R\mathcal{A}_R \\
&= -in_B(\mathcal{A}_L + \mathcal{A}_R) \\
&= -in_B\mathcal{A}.
\end{aligned}
\tag{A5}
$$

Then the Eq. (A2) can be re-written as

$$
\begin{aligned}
Q = \int \frac{d\varepsilon}{2\pi}\int \frac{d\omega}{2\pi}\hbar\omega \mathrm{Tr}[\mathrm{tr}\Big\{ & M[(f_L(\varepsilon)-1)A_L(\varepsilon) + (f_R(\varepsilon)-1)A_R(\varepsilon)]M \\
\times [f_L(\varepsilon-\hbar\omega)A_L(\varepsilon-\hbar\omega) + f_R(\varepsilon-\hbar\omega)A_R(\varepsilon-\hbar\omega)]\Big\} & n_B(\hbar\omega)\mathcal{A}(\omega)] \\
= \int \frac{d\varepsilon}{2\pi}\int \frac{d\omega}{2\pi}\hbar\omega \mathrm{Tr}[\mathrm{tr}\Big\{ & Q_0 \Big\} n_B(\hbar\omega)\mathcal{A}(\omega)]
\end{aligned}
\tag{A6}
$$

For simplicity, we set $Q_0 = Q_1 + Q_2 + Q_3 + Q_4$, where

$$
\begin{aligned}
Q_1 &= M(f_L(\varepsilon)-1)A_L(\varepsilon)Mf_L(\varepsilon-\hbar\omega)A_L(\varepsilon-\hbar\omega), \\
Q_2 &= M(f_L(\varepsilon)-1)A_L(\varepsilon)Mf_R(\varepsilon-\hbar\omega)A_R(\varepsilon-\hbar\omega), \\
Q_3 &= M(f_R(\varepsilon)-1)A_R(\varepsilon)Mf_L(\varepsilon-\hbar\omega)A_L(\varepsilon-\hbar\omega), \\
Q_4 &= M(f_R(\varepsilon)-1)A_R(\varepsilon)Mf_R(\varepsilon-\hbar\omega)A_R(\varepsilon-\hbar\omega).
\end{aligned}
\tag{A7}
$$

By introducing the mathematical relation

$$
[f(x)-\Theta(t)][f(y)-\Theta(-t)] = [\Theta(t)+n(x-y)][f(x)-f(y)]. \tag{A8}
$$

For our case

$$
[f_\alpha(\varepsilon)-1]f_\beta(\varepsilon-\hbar\omega) = [1+n(\hbar\omega+\mu_\beta-\mu_\alpha)][f_\alpha(\varepsilon)-f_\beta(\varepsilon-\hbar\omega)]. \tag{A9}
$$

Finally, we have

$$
Q = \sum_{\alpha\beta}\int \frac{d\varepsilon}{2\pi}\int \frac{d\omega}{2\pi}\hbar\omega \mathrm{Tr}[X_{\alpha\beta}(\varepsilon,\varepsilon-\hbar\omega)\mathcal{A}(\omega)]n_B(\hbar\omega)[n_B(\hbar\omega+\mu_\beta-\mu_\alpha)+1][f_\alpha(\varepsilon)-f_\beta(\varepsilon-\hbar\omega)], \tag{A10}
$$

where

$$
X_{\alpha\beta} = \mathrm{tr}[MA_\alpha MA_\beta(\varepsilon-\hbar\omega)]. \tag{A11}
$$

For $\alpha \neq \beta$

$$Q = \int \frac{d\omega}{2\pi} \hbar\omega \mathrm{Tr}[\Lambda_{LR} \mathcal{A}(\omega)][n_B(\hbar\omega; T) - n_B(\hbar\omega - eV; T)], \tag{A12}$$

where $eV = \mu_L - \mu_R$ and

$$\Lambda_{LR} = \int \frac{d\varepsilon}{2\pi} X_{LR}(\varepsilon, \varepsilon - \hbar\omega)[f_L(\varepsilon) - f_R(\varepsilon - \hbar\omega)]. \tag{A13}$$

Appendix B: The Hamiltonian for STM junction

For a STM junction as shown in Fig. (4), the Hamiltonian is

$$H = \underbrace{\sum_{k\nu=t,s} \varepsilon_{k\nu} c^\dagger_{k\nu} c_{k\nu} + \sum_{k\nu,k'\bar{\nu}} t_{\nu\bar{\nu}} (c^\dagger_{k\nu} c_{k'\bar{\nu}} + c^\dagger_{k'\bar{\nu}} c_{k\nu}) + \sum_{i=h,l} \varepsilon_i d^\dagger_i d_i + \sum_{i=h,l} \sum_{k\nu=s,t} t_{ik\nu} \left(d^\dagger_i c_{k\nu} + c^\dagger_{k\nu} d_i \right)}_{H_L}$$
$$+ \underbrace{\hbar\omega_0 \left(\frac{1}{2} + a^\dagger_0 a_0 \right)}_{H_B} + \underbrace{\sum_\alpha \hbar\omega_\alpha \left(\frac{1}{2} + b^\dagger_\alpha b_\alpha \right)}_{H_R} + \underbrace{m_0 (d^\dagger_h d_l a^\dagger_0 + d^\dagger_l d_h a_0)}_{H_{LB}} + \underbrace{\sum_\alpha t_\alpha (b^\dagger_\alpha a_0 + b_\alpha a^\dagger_0)}_{H_{BR}} . \tag{B1}$$

Based on the Hamiltonian, we can get the phtoton energy flux flowing from electron to photon subsystem. The expression of phtoton energy flux is similar to Eq. C4[28].

[1] T. Ojanen and A.-P. Jauho, Physical review letters **100**, 155902 (2008).

[2] J.-S. Wang, J. Wang, and N. Zeng, Physical Review B **74**, 033408 (2006).

[3] J.-S. Wang, N. Zeng, J. Wang, and C. K. Gan, Physical Review E **75**, 061128 (2007).

[4] J.-S. Wang, J. Wang, and J. Lü, The European Physical Journal B **62**, 381 (2008).

[5] T. Ruokola, T. Ojanen, and A.-P. Jauho, Physical Review B **79**, 144306 (2009).

[6] N. Li, J. Ren, L. Wang, G. Zhang, P. Hänggi, and B. Li, Reviews of Modern Physics **84**, 1045 (2012).

[7] E. Taylor and D. Segal, Physical review letters **117**, 220401 (2016).

[8] C.-H. Wang and J. M. Taylor, Physical Review B **94**, 155437 (2016).

[9] L. Zhang, J.-T. Lü, J.-S. Wang, and B. Li, Journal of Physics: Condensed Matter **25**, 445801 (2013).

[10] J. Ren, P. Hänggi, and B. Li, Physical review letters **104**, 170601 (2010).

[11] J. Ren, Physical Review B **82**, 155316 (2010).

[12] A. Nitzan and M. Ratner, The Journal of Physical Chemistry B **107**, 2377 (2003).

[13] R. Landauer, IBM Journal of Research and Development **1**, 223 (1957).

[14] M. Büttiker, Physical review letters **57**, 1761 (1986).

[15] Y. Meir and N. S. Wingreen, Physical review letters **68**, 2512 (1992).

[16] A.-P. Jauho, N. S. Wingreen, and Y. Meir, Physical Review B **50**, 5528 (1994).

[17] J.-T. Lü, R.-Q. Wang, and J.-S. Wang, Physical Review B **76**, 165418 (2007).

[18] M. Galperin, M. A. Ratner, and A. Nitzan, Journal of Physics: Condensed Matter **19**, 103201 (2007).

[19] H. Haug and A. P. Jauho, *Quantum kinetics in transport and optics of semiconductors* (Springer-Verlag: Berlin, 2008).

[20] M. Galperin and A. Nitzan, Physical Chemistry Chemical Physics **14**, 9421 (2012).

[21] J.-T. Lü, J.-S. Wang, P. Hedegård, and M. Brandbyge, Physical Review B **93**, 205404 (2016).

[22] X. Qiu, G. Nazin, and W. Ho, Science **299**, 542 (2003).

[23] G. Tian, J.-C. Liu, and Y. Luo, Physical review letters **106**, 177401 (2011).

[24] S.-E. Zhu, Y.-M. Kuang, F. Geng, J.-Z. Zhu, C.-Z. Wang, Y.-J. Yu, Y. Luo, Y. Xiao, K.-Q. Liu, Q.-S. Meng, *et al.*, Journal of the American Chemical Society **135**, 15794 (2013).

[25] G. Reecht, F. Scheurer, V. Speisser, Y. J. Dappe, F. Mathevet, and G. Schull, Physical review letters **112**, 047403 (2014).

[26] J. P. Bergfield and J. R. Hendrickson, Scientific reports **8**, 2314 (2018).

[27] P. Wurfel, Journal of Physics C: Solid State Physics **15**, 3967 (1982).

[28] L.-L. Nian, Y. Wang, and J.-T. Lü, Nano letters **18**, 6826 (2018).

[29] L. Yu, Z. K. Keane, J. W. Ciszek, L. Cheng, M. Stewart, J. Tour, and D. Natelson, Physical review letters **93**, 266802 (2004).

[30] Z. Huang, F. Chen, R. D'agosta, P. A. Bennett, M. Di Ventra, and N. Tao, Nature nanotechnology **2**, 698 (2007).

[31] Z. Ioffe, T. Shamai, A. Ophir, G. Noy, I. Yutsis, K. Kfir, O. Cheshnovsky, and Y. Selzer, Nature nanotechnology **3**, 727 (2008).

[32] R. Härtle and M. Thoss, Physical Review B **83**, 125419 (2011).

[33] L. Simine and D. Segal, Physical Chemistry Chemical Physics **14**, 13820 (2012).

[34] M. Galperin, K. Saito, A. V. Balatsky, and A. Nitzan, Physical Review B **80**, 115427 (2009).

[35] R. Härtle and M. Thoss, Physical Review B **83**, 115414 (2011).

[36] R. Härtle, C. Schinabeck, M. Kulkarni, D. Gelbwaser-Klimovsky, M. Thoss, and U. Peskin, Physical Review B **98**, 081404 (2018).

[37] R. I. Epstein, M. I. Buchwald, B. C. Edwards, T. R. Gosnell, and C. E. Mungan, Nature **377**, 500 (1995).

[38] L. Zhu, A. Fiorino, D. Thompson, R. Mittapally, E. Meyhofer, and P. Reddy, Nature **566**, 239 (2019).

[39] F. Herrmann and P. Würfel, American journal of physics **73**, 717 (2005).

[40] K. Chen, P. Santhanam, and S. Fan, Physical Review Applied **6**, 024014 (2016).

[41] Z.-Q. Zhang and J.-T. Lü, Physical Review B **96**, 125432 (

[42] P. Ben-Abdallah, Physical review letters **116**, 084301 (201

[43] P. Ben-Abdallah, Physical Review B **99**, 201406 (2019).

[44] A. Fiorino, D. Thompson, L. Zhu, R. Mittapally, S.-A. Bi S. Bansropun, P. Ben-Abdallah, E. Meyhofer, *et al.*, ACS